Report **Date** **Report number**
September 20, 2016 TRITA-EE 2016:142

Modelling the Dynamics of Energetic Ions and MHD Modes Influenced by ICRH

Emmi Tholerus, Thomas Johnson, and Torbjörn Hellsten
Department of Fusion Plasma Physics,
School of Electrical Engineering,
KTH Royal Institute of Technology,
100 44 Stockholm, SWEDEN
Email: emmi.tholerus@ee.kth.se

***Abstract*—FOXTAIL is a code used to describe the nonlinear interactions between toroidal Alfvén eigenmodes and an ensemble of resonant energetic particles in tokamaks with realistic geometries. This report introduces an extension of the code, including effects from ion cyclotron resonance heating (ICRH) of energetic ions using a quasilinear diffusion operator in adiabatic invariant space. First results of the effects of ICRH diffusion on the system consisting of a single Alfvén eigenmode linearly excited by resonant ions are presented. It is shown that the presence of ICRH diffusion allows for the mode amplitude to grow larger than in the case of nonlinear saturation in the absence of sources and sinks. Gradually increasing the strength of ICRH diffusion also decreases the linear growth rate of the mode. Both these phenomena are previously observed also for the case of a finite phase decorrelation operator in bump-on-tail systems with a single eigenmode.**

I. Introduction

THE toroidal geometry of the tokamak plasma induces frequency gaps in the shear Alfvén wave continuum as a result of coupling of poloidal harmonics. In these gaps, discrete frequency waves, so called toroidal Alfvén eigenmodes (TAEs), might exist [1], propagating with phase velocities $\omega/k \approx v_{\mathrm{A}} = B/\sqrt{\mu_0 \rho_{\mathrm{m}}}$. Light energetic ions have similar velocities, and can interact resonantly with TAEs. Inverted energetic ion distributions around the resonance can drive these modes unstable, especially considering that TAEs have comparably low instability thresholds [2]. Experiments have produced unstable TAEs driven by energetic ions coming from e.g. neutral beam injection (NBI) [3, 4], ion cyclotron resonance heating (ICRH) [5, 6], and from fusion born α-particles [7]. As the mode amplitudes grow large, their wave fields transport and potentially eject large fractions of energetic ions from the plasma, which reduces the possibility to achieve reactor relevant conditions significantly [3–7]. It is therefore of great importance to understand the mechanisms that excite and govern the dynamics of these modes.

Many of the important properties of the TAE dynamics, such as amplitude saturation and frequency chirping, are understood to be dependent on the nonlinear dynamics of TAEs and energetic ions. Understanding the long time scale dynamics of these systems could also be much relevant for future devices, such as ITER, because of long pulse operation and the importance of sufficient α-particle heating. FOXTAIL [8] is a code designed to simulate the long time scale nonlinear dynamics of TAEs and ensembles of energetic ions in realistic tokamak geometries.

This report also presents an extension of the code, consisting of a quasilinear diffusion operator modelling the influence of ICRH on the dynamics of TAEs and energetic ions. To the authors' best knowledge, few numerical modelling studies aimed at describing TAE–energetic ion dynamics specifically under the influence of ICRH have been made. Studies of a numerical model for TAE–ion dynamics during ICRH were made by Bergkvist, *et al.* [9, 10]. The studies showed mode damping on time scales faster than the slowing down time as the ICRH is deactivated, and pitch-fork splitting of the mode frequency by renewal of the tail distribution by ICRH, which is in agreement with experimental observations [11, 12]. However, the numerical model for the TAE–energetic ion interaction used in the studies was quasilinear. Presented in this report is a fully nonlinear interaction model, with the ability to simulate scenarios with wave–particle interactions weakly decorrelated by the presence of ICRH.

The structure of the report is as follows: Section II presents a description of FOXTAIL and of the quasilinear ICRH operator. Section III presents the studies made for this report, starting with the description of a more specific ICRH diffusion operator used in the studies. This is followed by a presentation of the parameter setup for the simulations and numerical results from these. The studies investigates the dynamics of a single TAE interacting with an energetic bump-on-tail distribution under the influence of the suggested ICRH diffusion operator at various diffusion strengths, from weak to strong decorrelation of the interaction. Section IV presents the main conclusions made in the report.

II. Model description

A. Overview of FOXTAIL

FOXTAIL is a Monte Carlo model, where the energetic particles are represented by discrete markers in a 5D phase space. Three of the phase space coordinates are the invariants E (kinetic energy), P_ϕ (toroidal canonical momentum) and μ (magnetic moment, which is an adiabatic invariant). The remaining two coordinates are the transformed poloidal ($\tilde{\theta}$) and toroidal ($\tilde{\phi}$) angles, part of an action–angle canonical coordinate system [13] of the equilibrium (i.e., in the absence of TAEs).

The equations of motion of the system are given by

$$\begin{cases} \dot{E}_k = \mathrm{Re}\sum_i A_i U_{i,k}, & \dot{\tilde{\theta}}_k = \omega_\mathrm{B}(\boldsymbol{J}_k), \\ \dot{P}_{\phi,k} = \mathrm{Re}\sum_i \frac{n_i}{\omega_i} A_i U_{i,k}, & \dot{\tilde{\phi}}_k = \omega_\mathrm{p}(\boldsymbol{J}_k), \\ \dot{\mu}_k = 0, & \dot{A}_i = -\sum_k w_k U^*_{i,k}, \end{cases} \tag{1}$$

where

$$U_{i,k} \equiv \sum_\ell V_{i,\ell}(\boldsymbol{J}_k) \mathrm{e}^{\mathrm{i}(\ell\tilde{\theta}_k + n_i\tilde{\phi}_k - \omega_i t)}, \tag{2}$$

and $\boldsymbol{J}_k \equiv (E_k, \mu_k, P_{\phi,k})$. Here, A_i is the amplitude of the i:th mode, normalised such that $|A_i|^2/2$ is the mode energy, and n_i and ω_i are the toroidal mode number and frequency of the same mode, respectively. The index k labels each marker representing the energetic particle distribution, with a weight factor w_k. The frequencies ω_B and ω_p are the bounce and precession frequencies of the particle. The fields $V_{i,\ell}(\boldsymbol{J})$ are Fourier coefficients in $\tilde{\theta}$-space of a function quantifying the instantaneous acceleration of a particle interacting with a single eigenmode (see Ref. [8] for details). FOXTAIL solves eq. (1) for a set of markers and mode amplitudes using the standard 4th order Runge–Kutta method.

Equation (1) only includes direct eigenmode–energetic particle interaction, and it excludes particle collisions, eigenmode damping (coming e.g. from interaction with a thermal distribution or damping in connection with mode conversion) and particle sources and sinks (auxiliary heating, Bremsstrahlung, fusion reactions, etc.). The next section presents an extension of the FOXTAIL model, which includes a quasilinear diffusion operator modelling the effects of ion cyclotron resonance heating (ICRH).

B. Quasilinear ICRH operator

References [14, 15] present an ICRH operator acting on an ion species. The operator, averaged over the guiding centre orbits of the ions, can be expressed as

$$\left.\frac{\mathrm{d}f}{\mathrm{d}t}\right|_\mathrm{RF} = \sum_{n_\mathrm{h},n_\mathrm{a},\omega_\mathrm{a}} \mathcal{L}(D_\mathrm{RF}\mathcal{L}(f)), \tag{3}$$

where

$$\mathcal{L} = \frac{\partial}{\partial E} + \frac{1}{B_\mathrm{res}}\frac{\partial}{\partial \mu} + \frac{n_\mathrm{a}}{\omega_\mathrm{a}}\frac{\partial}{\partial P_\phi}, \tag{4}$$

$$D_\mathrm{RF} = \frac{\omega_\mathrm{B}}{8\pi}\sum_{n_\mathrm{r}} \left| Zev_\perp(\mathcal{E}_+ J_{n_\mathrm{h}-1} + \mathrm{e}^{2\mathrm{i}\zeta}\mathcal{E}_- J_{n_\mathrm{h}+1})\Pi \right|^2. \tag{5}$$

Here, ω_a and n_a are the frequency and toroidal mode number of the ICRH wave field, n_h is the harmonic number of the ion cyclotron resonance, $B_\mathrm{res} = m\omega_\mathrm{a}/Ze$ is the resonant magnetic field of the fundamental resonance, $\mathcal{E}_+$ and $\mathcal{E}_-$ are the left- and right-hand polarized components of the electric wave field, respectively, and ζ is the angle of propagation of the wave in the plane perpendicular to the magnetic field. $J_{n_\mathrm{h}\pm1}$ are Bessel functions of the first kind with the argument $k_\perp v_\perp/\Omega_\mathrm{c}$. n_r indexes the locations of the local ion cyclotron resonances $\dot{\nu} = 0$ along the orbit, where ν is the relative phase of the gyro-orbit and left-hand component of the electric wave field, calculated by

$$\nu(t) = \nu(t_0) + \int_{t_0}^{t} \mathrm{d}t'(\omega_\mathrm{a} - n_\mathrm{h}\Omega_\mathrm{c} - k_\parallel v_\parallel - \boldsymbol{k}_\perp \cdot \boldsymbol{v}_\mathrm{d}), \tag{6}$$

with $\boldsymbol{v}_\mathrm{d}$ being the perpendicular drift velocity of the ion. The number of local resonances varies between 0 and 4 in different regions in momentum space. Π in eq. (5) is the phase integral:

$$\Pi = \int \mathrm{d}t\, \mathrm{e}^{\mathrm{i}\nu(t)} \approx \sqrt{\frac{2\pi\mathrm{i}}{\ddot{\nu}}}\mathrm{e}^{\mathrm{i}\nu}. \tag{7}$$

The approximation in eq. (7), being the phase integral evaluated at the local ion cyclotron resonance, results from expanding ν to second order in t. The approximation lacks validity in a neighbourhood around $\ddot{\nu} = 0$, where the inclusion of higher order terms is required [16]. The diffusion coefficient of eq. (5) was derived assuming that the phase ν is decorrelated each time the ion passes the local resonance, e.g. by collisions or by nonlinear effects.

III. The effects of ICRH diffusion

A. The ICRH diffusion operator

The aim of the presented study is to investigate how the TAE dynamics is qualitatively affected by an energetic ion distribution under the influence of ICRH diffusion. The operator of eq. (3) includes some physical properties that are not necessary to account for in this particular study. Consequently, a set of simplifying assumptions are made for the FOXTAIL implementation of the ICRH diffusion operator. The first assumption is that only one single antenna is present with a single toroidal mode number, removing the summation over n_a and ω_a in eq. (3). Furthermore, the transferred toroidal kinetic momentum from the ICRH wave field to the ions ($\partial/\partial P_\phi$ term in eq. (4)) and the Doppler shift (velocity dependent terms in the resonance condition) are neglected. We choose also only to consider the fundamental cyclotron resonance ($n_\mathrm{h} = 1$). Then, given that $k_\perp v_\perp/\Omega_\mathrm{c} \ll 1$, the Bessel function $J_{n_\mathrm{h}+1} = J_2$ is negligible compared to $J_{n_\mathrm{h}-1} = J_0 \approx 1$, and the second term of eq. (5) can be neglected. It is also assumed that the energetic ion distribution is sufficiently far from the point where $\ddot{\nu} = 0$ at the local resonances, making the approximation of eq. (7) valid. Consequently, the operator is given by the equation

$$\left.\frac{\mathrm{d}f}{\mathrm{d}t}\right|_\mathrm{RF} = \mathcal{L}(D_\mathrm{RF}\mathcal{L}(f)), \tag{8}$$

with

$$\mathcal{L} = \frac{\partial}{\partial E} + \frac{1}{B_\mathrm{res}}\frac{\partial}{\partial \mu}, \tag{9}$$

$$\begin{aligned} D_\mathrm{RF} &= \frac{\omega_\mathrm{B}}{4}\sum_{n_\mathrm{r}} \frac{|Zev_\perp\mathcal{E}_+|^2}{|\dot{\Omega}_\mathrm{c}|} \\ &= \frac{Ze\omega_\mathrm{B}|\mathcal{E}_+|^2\mu B_\mathrm{res}}{2}\sum_{n_\mathrm{r}}\frac{1}{|\dot{B}|}. \end{aligned} \tag{10}$$

The derivatives $\dot{\Omega}_\mathrm{c}$ and $\dot{B}$ are calculated along the unperturbed guiding centre orbit and evaluated at the resonant points $\omega_\mathrm{a} = \Omega_\mathrm{c}$ (which is equivalent to $B = B_\mathrm{res}$). It can be

seen that the points in momentum space where $\dot{B} = 0$, the diffusion coefficient becomes singular, as a consequence of the approximation of eq. (7). For trapped ions, this happens for instance at the surface $E = \mu B_{\mathrm{res}}$.

In order to implement the ICRH operator in FOXTAIL, the operator should be written on the form of a system of differential equations describing the motion of individual markers, as in eq. (1). In Ref. [15], a system of stochastic differential equations (SDEs) in E,Λ,P_ϕ-space is given on Itō form for each marker, where $\Lambda \equiv \mu B_0/E$ is the normalized magnetic moment and B_0 is the on-axis magnetic field strength. With the assumptions used for the ICRH operator in this report, the system of SDEs reads

$$\begin{cases} \mathrm{d}E_{\mathrm{RF}} = \mathcal{L}D_{\mathrm{RF}}\,\mathrm{d}t + \sqrt{2D_{\mathrm{RF}}}\,\mathrm{d}W_t, \\ \mathrm{d}\Lambda_{\mathrm{RF}} = \dfrac{\Lambda_{\mathrm{res}} - \Lambda}{E}\left(\mathcal{L}D_{\mathrm{RF}} - \dfrac{2D_{\mathrm{RF}}}{E}\right)\mathrm{d}t \\ \qquad\qquad + \dfrac{\Lambda_{\mathrm{res}} - \Lambda}{E}\sqrt{2D_{\mathrm{RF}}}\,\mathrm{d}W_t, \\ \mathrm{d}P_{\phi,\mathrm{RF}} = 0, \end{cases} \tag{11}$$

where $\Lambda_{\mathrm{res}} = B_0/B_{\mathrm{res}}$ corresponds to the singular surface $E = \mu B_{\mathrm{res}}$, and W_t is a Wiener process. Using Itō's lemma, this system of SDEs can be transformed to coordinates (E, μ, P_ϕ):

$$\begin{cases} \mathrm{d}E_{\mathrm{RF}} = \mathcal{L}D_{\mathrm{RF}}\,\mathrm{d}t + \sqrt{2D_{\mathrm{RF}}}\,\mathrm{d}W_t, \\ \mathrm{d}\mu_{\mathrm{RF}} = \dfrac{1}{B_{\mathrm{res}}}\mathcal{L}D_{\mathrm{RF}}\,\mathrm{d}t + \dfrac{1}{B_{\mathrm{res}}}\sqrt{2D_{\mathrm{RF}}}\,\mathrm{d}W_t, \\ \mathrm{d}P_{\phi,\mathrm{RF}} = 0. \end{cases} \tag{12}$$

It can be seen from eq. (12) that the total power transferred from the antenna to the simulated fraction of energetic particles is on average given by

$$P_{\mathrm{RF}} = \sum_k \mathcal{L}D_{\mathrm{RF}}(\boldsymbol{J}_k)w_k. \tag{13}$$

In the presented version of the ICRH operator, the diffusion coefficient of eq. (10) is taken to be constant. With this simplification, the average power transfer P_{RF} vanishes. It is computationally simpler, since one does not have to evaluate the diffusion coefficient at each of the marker locations in momentum space throughout the simulation. A reference point in phase space is chosen where the diffusion coefficient is evaluated, giving the correct ordering of the ICRH diffusion. The reference point is chosen to be located within the region of the initial distribution function.

Using the Euler–Maruyama numerical scheme and assuming a constant D_{RF}, a finite time step Δt evolves the markers in E,μ-space according to

$$\begin{cases} E_{k,m+1} = E_{k,m} + \zeta_{k,m}\sqrt{2D_{\mathrm{RF}}\Delta t}, \\ \mu_{k,m+1} = \mu_{k,m} + \zeta_{k,m}\dfrac{\sqrt{2D_{\mathrm{RF}}\Delta t}}{B_{\mathrm{res}}}, \end{cases} \tag{14}$$

where $\zeta_{k,m}$ are normally distributed random variables of unit variance, k is the marker index and m is the time index. The random terms of eq. (14) are added to FOXTAIL for each marker after each Runge–Kutta time step solving the interaction between energetic particles and TAEs.

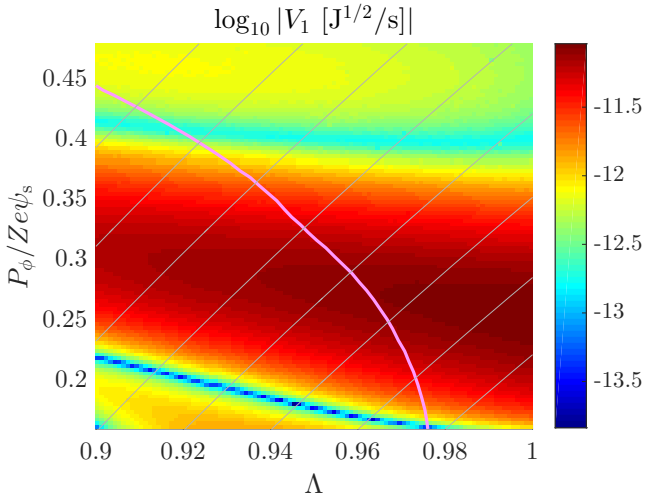

Figure 1. The interaction coefficient $V_{\ell=1}$ in Λ,P_ϕ-space, at $\mu = 300\,\mathrm{keV/T}$. The pink curve is the wave–particle resonance $\ell\omega_{\mathrm{B}} + n\omega_{\mathrm{p}} = \omega_{\mathrm{TAE}}$ for $(\ell, n) = (1, 4)$. The thin grey curves are the characteristic curves for wave–particle interaction, defined by $E + (\omega_{\mathrm{TAE}}/n)P_\phi = \mathrm{const.}$ ψ_{s} is the value of poloidal magnetic flux per radian on the separatrix. Consequently, $P_\phi/Ze\psi_{\mathrm{s}}$ is the approximate value of $s^2 = \psi/\psi_{\mathrm{s}}$ at the turning point $v_\parallel = 0$ of the orbit.

B. Simulation parameters

In the presented studies, a system is chosen containing an ensemble of energetic $^3\mathrm{He}^{2+}$ ions close to the resonance of a single TAE. The equilibrium is calculated with the CHEASE code [17], using a JET-like configuration with on-axis magnetic field $B_0 = 2.4\,\mathrm{T}$ and core electron temperature $T_{\mathrm{e},0} = 5.7\,\mathrm{keV}$. The included TAE has a toroidal mode number of $n = 4$, and poloidal mode numbers $m = [5, 6]$. Eigenfunctions of the TAE are calculated analytically using the method described in Ref. [18].

The FOXTAIL simulations presented in this report only considers the dynamics of energetic particles in an adiabatic invariant space spanned by $0.9 \leq \Lambda \leq 1$, $0.3\,\mathrm{eVs} \leq P_\phi \leq 0.9\,\mathrm{eVs}$ (which corresponds to $0.16 \leq P_\phi/Ze\psi_{\mathrm{s}} \leq 0.48$), $250\,\mathrm{keV/T} \leq \mu \leq 350\,\mathrm{keV/T}$. In this invariant space, all $^3\mathrm{He}^{2+}$ ions are trapped ($v_\parallel$ changes sign along the orbit). Markers crossing the boundaries of the simulated invariant space are reflected at the boundary surface.

A single Fourier coefficient of the interaction coefficient V_ℓ is included: $\ell = 1$ (mode index i is suppressed since the system only contains one mode). This interaction coefficient is plotted in Fig. 1 in Λ,P_ϕ-space, along with the resonance and the characteristic curves for eigenmode–particle interaction. An energetic particle distribution, consisting of 10^{15} $^3\mathrm{He}^{2+}$ ions distributed on 10^6 markers, is placed in relation to the resonance such that there is a positive derivative of the energy distribution function at the resonance along the characteristic curves of wave–particle interaction (see Fig. 2). Such a placement initially transfers net energy from the energetic particles to the TAE via a process analogous to Landau damping. The distribution is a Gaussian along the characteristic curves and along the resonance surface. As the mode amplitude grows, the regions of phase space around the resonance where the ions are trapped by the wave field grows wider in energy.

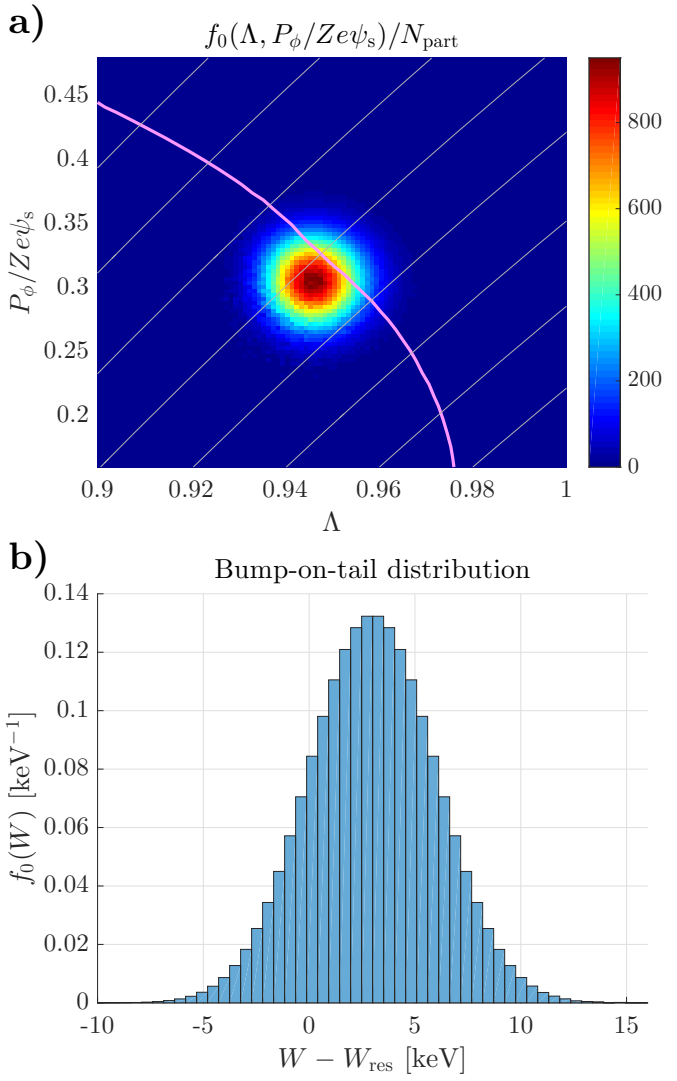

Figure 2. a) Initial energetic particle distribution function in Λ,P_ϕ-space (all remaining dimensions of the distribution function are integrated over) along with the resonance (pink curve) and the curves for wave–particle interaction (grey curves). b) Corresponding "bump-on-tail" distribution, i.e., the distribution of the energy difference between the particles and the resonance surface ($\ell\omega_{\rm B} + n\omega_{\rm p} = \omega_{\rm TAE}$) along the characteristic curves for wave–particle interaction (see Ref. [8] for details).

The mixing of ions inside the separatrices locally flattens the energy distribution around the wave–particle resonance, gradually braking the growth of the mode amplitude. Eventually, the mode is expected to reach a saturated state, where the ion energy distribution is completely flattened around the resonance.

The quasilinear ICRH operator is configured such that the antenna frequency matches the ^{3}He^{2+} cyclotron frequency at the magnetic axis ($B_{\rm res} = B_0$ and $\omega_{\rm a}/2\pi \approx 24\,$MHz). The singular surface of the ICRH diffusion coefficient, $E = \mu B_{\rm res}$, then corresponds to the surface $\Lambda = B_0/B_{\rm res} = 1$. Figure 3 shows the diffusion coefficient of eq. (10) calculated at the simulated part of Λ,P_ϕ-space. A reference point where $D_{\rm RF}$ is evaluated is chosen at $(\Lambda, P_\phi, \mu) = (0.95, 0.6\,{\rm eVs} = 0.32 Ze\psi_{\rm s}, 300\,{\rm keV/T})$. When the left-handed electric ICRH wave field component is chosen to be 200 V/m, the diffusion

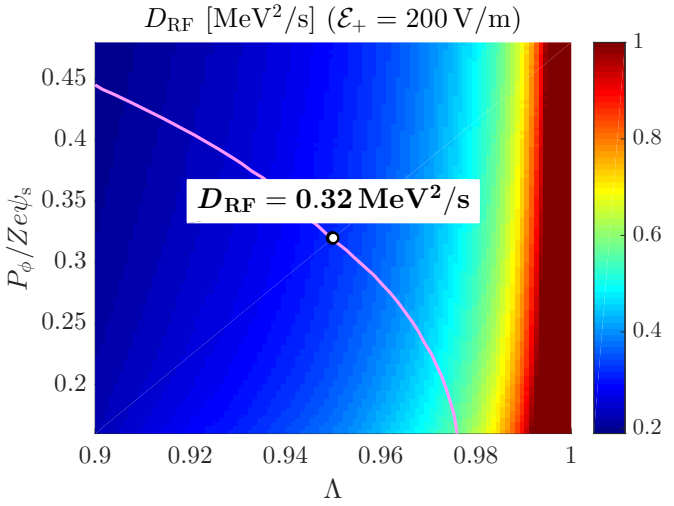

Figure 3. The ICRH diffusion coefficient of eq. (10) at $\mu = 300\,$keV/T. The colour scale of $D_{\rm RF}$ has an upper bound at 1 MeV^2/s, although the diffusion coefficient has far larger values close to the singularity at $\Lambda = 1$. The white dot shows the location of the reference point, where the constant value of $D_{\rm RF}$ used in the simulations is evaluated.

coefficient in the reference point has the value $D_{\rm RF} = 0.32\,{\rm MeV^2/s}$.

In order to relate the strength of the diffusion coefficient with a specific antenna power, a simple power absorption model is used [19]. According to this model, the ICRH wave field can be parted in a weakly damped and a strongly damped component. It is here assumed, for simplicity, that the weakly damped component is homogeneous in field strength throughout the plasma, whereas the strongly damped component is localized in the core of the plasma. The width of the strongly damped component around the magnetic axis for on-axis heating depends on the Doppler broadening of the cyclotron resonance and on the focusing of the antenna. The simulated fraction of energetic ions is centered around $s = \sqrt{\psi/\psi_{\rm s}} \approx 0.57$, being well outside the localized wave field of the strongly damped component for typical plasma parameters. Consequently, the weakly damped wave field component dominates in this region. From the homogeneity of the weakly damped wave field component, it can be further assumed that the power transmitted to the simulated fraction of ions has the same average power transmission per ion as the remaining part of the ^{3}He^{2+} ions heated by the weakly damped component.

The power transmitted to the simulated fraction of energetic ions is 110 W, which is found from eq. (13) by evaluating $D'_{\rm RF}$ numerically for $\mathcal{E}_+ = 200\,$V/m and summing over the initial ^{3}He^{2+} distribution. The width of power absorption, ΔR, around the resonance $R = R_0$ is estimated by

$$k_\parallel v_\parallel = \omega_{\rm a} - \Omega_{\rm c}(R_0 + \Delta R/2) \approx \omega_{\rm a}\left(1 - \frac{R_0}{R_0 + \Delta R/2}\right),$$

where $R_0 \approx 3\,$m is the major radius. Using $k_\parallel = 25/R_0$ and $v_\parallel \approx v_{\rm th}/\sqrt{2} \approx 5.2 \times 10^5\,$m/s gives an absorption width of $\Delta R \approx 17\,$cm. The volume of absorption is then $V = 2\pi h R_0 \Delta R = 8.8\,{\rm m}^3$, assuming a height $h = 2.8\,$m. Given an average ^{3}He^{2+} ion density of $1 \times 10^{18}\,{\rm m}^{-3}$, the total

amount of heated $^3He^{2+}$ ions is 8.8×10^{18}. The total power transmitted by the weakly damped field component is then

$$P_{\mathrm{weak}} = 110\,\mathrm{W} \times \frac{8.8 \times 10^{18}}{1 \times 10^{15}} = 960\,\mathrm{kW}.$$

The fraction of the total power transmitted by the weakly damped component can be related to the single pass damping of the wave, a_s, according to

$$P_{\mathrm{weak}} = (1 - a_s(2 - a_s))P_{\mathrm{tot}}. \quad (15)$$

If a 20 %, a 50 % or a 80 % single pass damping is assumed, then the total ICRH power is 1.5 MW, 3.9 MW or 24 MW, respectively. Hence, whether the assumed left-hand polarized electric field component $\mathcal{E}_+ = 200$ V/m is reasonable depends primarily on the damping of the wave.

C. Scan of ICRH diffusion strength

In these studies, the value of the diffusion coefficient is varied around the reference value of $D_{\mathrm{RF,ref}} = 0.32\,\mathrm{MeV}^2/\mathrm{s}$. We introduce a proportionality constant d such that $D_{\mathrm{RF}} = d \times D_{\mathrm{RF,ref}}$. The amplitude evolution of the TAE for a wide range of proportionality constants is plotted in Fig. 4, and the final bump-on-tail distributions of the energetic particles for a subset of the studied cases is shown in Fig. 5.

We note first that in the absence of ICRH diffusion, the mode grows exponentially and nonlinearly saturates at around $\delta B/B_0 = 3 \times 10^{-4}$, with a corresponding local flattening of the bump-on-tail distribution around the resonance. These growth and saturation mechanisms are well studied phenomena in bump-on-tail models (see e.g. Refs.[20, 21]), and connected to the evolution of TAEs via the theory of Berk *et al.* [22, 23], on which the FOXTAIL model is based. The mode growth and saturation are modified as the proportionality constant is gradually increased. In the presence of ICRH diffusion, the mode does not appear to saturate at the considered time scales. It can grow larger than in the absence of diffusion, which is explicitly seen for $0.001 \leq d \leq 0.2$ in Fig. 4. For $d \gtrsim 0.1$, the growth rate of the mode decreases significantly with increasing diffusion strength. Above $d = 1$, the mode amplitude is strongly damped on the studied time scales. An effect on the energy distribution function by the presence of ICRH diffusion is a broadening of the whole distribution around the resonance, as seen in Fig. 5.

Similar dynamics of the mode amplitude and the bump-on-tail distribution has been observed in a bump-on-tail model in the presence of phase decorrelation [24]. In the presence of phase decorrelation, the mode saturates at an amplitude where the energy transferred from the energetic particles to the wave is the energy difference between the initial energetic particle distribution and a final distribution corresponding to a symmetric distribution around the resonance. As the phase decorrelation is increased, the saturation amplitude is maintained, but the growth rate gradually decreases. The theoretical saturation amplitude for the TAE by the presence of phase decorrelation in the cases presented in this report is $\delta B/B_0 = 1.3 \times 10^{-3}$. Although not explicitly shown by the results of Fig. 4, it is possible that this is the saturation amplitude of the mode also

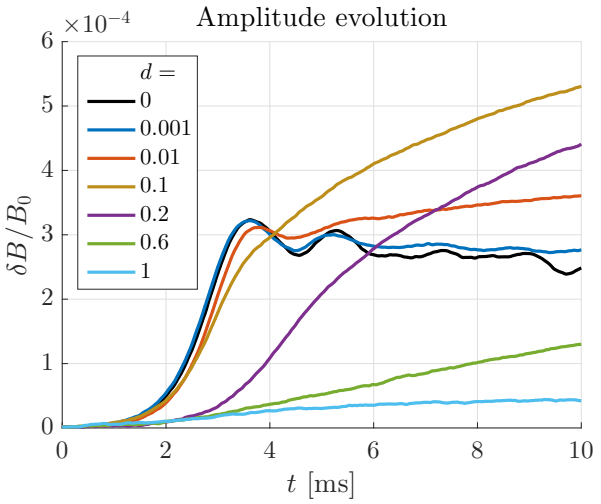

Figure 4. The evolution of the TAE amplitude for a set of proportionality constants d relative to the reference value of ICRH diffusion $D_{\mathrm{RF,ref}} = 0.32\,\mathrm{MeV}^2/\mathrm{s}$. δB is the local maximum of the magnetic wave field around the $q(\psi) = (5 + \frac{1}{2})/4$ surface, where q is the safety factor.

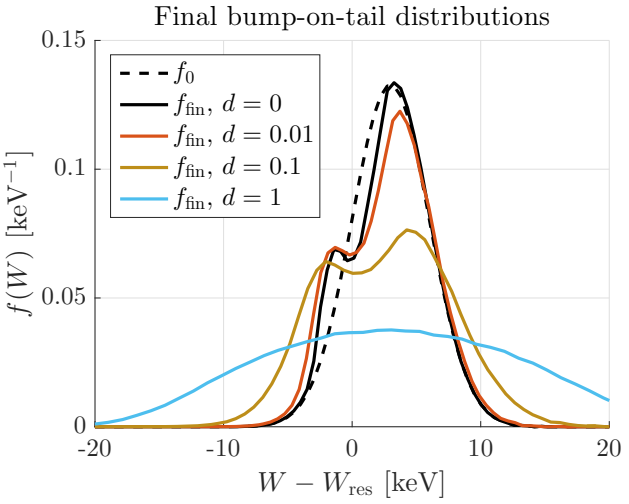

Figure 5. The initial bump-on-tail distribution (dashed curve) and final bump-on-tail distributions (solid curves, evaluated at $t = 10$ ms) for a subset of the cases presented in Fig. 4.

in the presence of ICRH diffusion. This conjecture is based on the argument that the suggested ICRH diffusion operator is energy conserving on average, and the energy difference between the initial state and a final symmetric bump-on-tail distribution corresponds to the maximum exhaustible energy from the energetic ion distribution to the TAE in the absence of sources and sinks. Such a state cannot be reached in the absence of decorrelation processes in general, because of coherent dynamics prohibiting the leaking of particles through the separatrices of the wave field in particle phase space. The suggested final state is not expected to be unique for the case of finite phase decorrelation, but in principle *any* energy conserving process that decorrelates the interaction between energetic particles and a single TAE in the absence of sources and sinks. However, having a non-constant interaction coefficient $V_{i,\ell}$ along the characteristic curves of wave–particle

interaction, which is the case for the FOXTAIL model, but not for the bump-on-tail model presented in Ref. [24], might also break the symmetry of the theoretical final state, perturbing the saturated mode energy. Note also that the more realistic ICRH operator is not energy conserving (otherwise there would be no heating!). The similarities with the effects of phase decorrelation is interesting more from the point of view that this is a mathematically different decorrelation process, indicating that the effects of phase decorrelation, as studied in Ref. [24], occur qualitatively also for other decorrelation processes.

IV. Conclusions

The original FOXTAIL code [8], used to simulate the nonlinear interaction between toroidal Alfvén eigenmodes (TAEs) and resonant energetic ions, has been extended to include a diffusion operator modelling the effects of ion cyclotron resonance heating (ICRH). Based on the quasilinear ICRH operator presented in Ref. [14], the operator described in this report uses a set of simplifying assumptions to arrive at a constant diffusion operator in kinetic energy and magnetic moment. The suggested simplifications conserves the total energy of the system on average.

A test case has been constructed without any sources or sinks, in which an ensemble of energetic $^3He^{2+}$ ions excites and nonlinearly saturates a single TAE. The positive derivative of the ion energy distribution along the characteristic curves of wave–particle interaction at the resonance transfers net energy from the ions to the TAE. As ions mix inside the regions of phase space where they are trapped by the TAE wave field, the energy distribution is locally flattened around the resonance, and the eigenmode nonlinearly saturates.

As the ICRH diffusion operator is included in the system, the mode amplitude does no longer saturate on the studied time scales. Above a certain threshold of the value of the ICRH diffusion coefficient, the growth rate of the mode decreases significantly with the increasing diffusion coefficient. These observed effects are a lot reminiscent of the effects of phase decorrelation in bump-on-tail models [24]. One of the major differences between phase decorrelation and ICRH diffusion is that mode amplitude saturation typically takes place on time scales similar to the inverse linear growth rate in the presence of phase decorrelation, whereas it appears to take place on longer time scales for finite ICRH diffusion.

The saturated state for a system with finite phase decorrelation is a state where the energy transferred from the energetic particles to the wave is the energy difference between the initial energetic particle distribution and a final state corresponding to a symmetric distribution in energy around the resonance. Although it was not explicitly shown by the results of this report, it is possible that this saturated state is the same also in the presence of finite ICRH diffusion, in the special case of an energy conserving operator on average. The varying interaction strength between the energetic ions and the TAE in different part of momentum space might perturb the saturated mode energy in the presence of ICRH diffusion, assuming that these variations produce asymmetrical final bump-on-tail distributions around the wave–particle resonance.

References

[1] C. Z. Cheng and M. S. Chance, "Low-n shear Alfvén spectra in axisymmetric toroidal plasmas," *Phys. Fluids*, vol. 29, no. 11, pp. 3695 – 3701, 1986, doi:10.1063/1.865801.

[2] G. Y. Fu and J. W. Van Dam, "Excitation of the toroidicity-induced shear Alfvén eigenmode by fusion alpha particles in an ignited tokamak," *Phys. Fluids B*, vol. 1, no. 10, pp. 1949 – 1952, 1989, doi:10.1063/1.859057.

[3] K. L. Wong, R. J. Fonck, S. F. Paul, D. R. Roberts, E. D. Fredrickson, R. Nazikian, H. K. Park, M. Bell, N. L. Bretz, R. Budny, S. Cohen, G. W. Hammett, F. C. Jobes, D. M. Meade, S. S. Medley, D. Mueller, Y. Nagayama, D. K. Owens, and E. J. Synakowski, "Excitation of Toroidal Alfvén Eigenmodes in TFTR," *Phys. Rev. Lett.*, vol. 66, no. 14, pp. 1874 – 1877, 1991, doi:10.1103/PhysRevLett.66.1874.

[4] W. W. Heidbrink, E. J. Strait, E. Doyle, G. Sager, and R. T. Snider, "An investigation of beam driven Alfvén instabilities in the DIII-D tokamak," *Nucl. Fusion*, vol. 31, no. 9, pp. 1635 – 1648, 1991, doi:10.1088/0029-5515/31/9/002.

[5] K. L. Wong, J. R. Wilson, Z. Y. Chang, G. Y. Fu, E. Fredrickson, G. W. Hammett, C. Bush, C. K. Phillips, J. Snipes, and G. Taylor, "Expansion of parameter space for toroidal Alfvén eigenmode experiments in TFTR," *Plasma Phys. Control. Fusion*, vol. 36, no. 5, pp. 879 – 895, 1994, doi:10.1088/0741-3335/36/5/009.

[6] S. Ali-Arshad and D. J. Campbell, "Observation of TAE activity in JET," *Plasma Phys. Control. Fusion*, vol. 37, no. 7, pp. 715 – 722, 1995, doi:10.1088/0741-3335/37/7/002.

[7] R. Nazikian, G. Y. Fu, S. H. Batha, M. G. Bell, R. E. Bell, R. V. Budny, C. E. Bush, Z. Chang, Y. Chen, C. Z. Cheng, D. S. Darrow, P. C. Efthimion, E. D. Fredrickson, N. N. Gorelenkov, B. Leblanc, F. M. Levinton, R. Majeski, E. Mazzucato, S. S. Medley, H. K. Park, M. P. Petrov, D. A. Spong, J. D. Strachan, E. J. Synakowski, G. Taylor, S. von Goeler, R. B. White, K. L. Wong, and S. J. Zweben, "Alpha-Particle-Driven Toroidal Alfvén Eigenmodes in the Tokamak Fusion Test Reactor," *Phys. Rev. Lett.*, vol. 78, no. 15, pp. 2976 – 2979, 1997, doi:10.1103/PhysRevLett.78.2976.

[8] E. Tholerus, T. Johnson, and T. Hellsten, "FOXTAIL: Modeling the nonlinear interaction between Alfvén eigenmodes and energetic particles in tokamaks," submitted to *Comput. Phys. Commun.* in June, 2016. Preprint (not accepted for publication) is available at https://arxiv.org/abs/1607.04561.

[9] T. Bergkvist, T. Hellsten, T. Johnson, and M. Laxåback, "Non-linear study of fast particle excitation of Alfvén eigenmodes during ICRH," *Nucl. Fusion*, vol. 45, no. 6, pp. 485 – 493, 2005, doi:10.1088/0029-5515/45/6/010.

[10] T. Bergkvist, T. Hellsten, and K. Holmström, "Non-linear dynamics of Alfvén eigenmodes excited by thermonu-

clear alpha particles in the presence of ion cyclotron resonance heating," *Nucl. Fusion*, vol. 47, no. 9, pp. 1131 – 1141, 2007, doi:10.1088/0029-5515/47/9/009.

[11] K. L. Wong, R. Majeski, M. Petrov, J. H. Rogers, G. Schilling, J. R. Wilson, H. L. Berk, B. N. Breizman, M. Pekker, and H. V. Wong, "Evolution of toroidal Alfvén eigenmode instability in Tokamak Fusion Test Reactor," *Phys. Plasmas*, vol. 4, no. 2, pp. 393 – 404, 1997, doi:10.1063/1.872098.

[12] A. Fasoli, B. N. Breizman, D. Borba, R. F. Heeter, M. S. Pekker, and S. E. Sharapov, "Nonlinear Splitting of Fast Particle Driven Waves in a Plasma: Observation and Theory," *Phys. Rev. Lett.*, vol. 81, no. 25, pp. 5564 – 5567, 1998, doi:10.1103/PhysRevLett.81.5564.

[13] A. N. Kaufman, "Quasilinear diffusion of an axisymmetric toroidal plasma," *Phys. Fluids*, vol. 15, no. 6, pp. 1063 – 1069, 1972, doi:10.1063/1.1694031.

[14] T. Johnson, T. Hellsten, and L.-G. Eriksson, "Analysis of a quasilinear model for ion cyclotron interactions in tokamaks," *Nucl. Fusion*, vol. 46, no. 7, pp. S433 – S441, 2006, doi:10.1088/0029-5515/46/7/S06.

[15] L.-G. Eriksson, M. J. Mantsinen, T. Hellsten, and J. Carlsson, "On the orbit-averaged Monte Carlo operator describing ion cyclotron resonance frequency wave–particle interaction in a tokamak," *Phys. Plasmas*, vol. 6, no. 2, pp. 513 – 518, 1999, doi:10.1063/1.873195.

[16] G. D. Kerbel and M. G. McCoy, "Kinetic theory and simulation of multispecies plasmas in tokamaks excited with electromagnetic waves in the ion-cyclotron range of frequencies," *Phys. Fluids*, vol. 28, no. 12, pp. 3629 – 3653, 1985, doi:10.1063/1.865319.

[17] H. Lütjens, A. Bondeson, and O. Sauter, "The CHEASE code for toroidal MHD equilibria," *Comput. Phys. Commun.*, vol. 97, no. 3, pp. 219 – 260, 1996, doi:10.1016/0010-4655(96)00046-X.

[18] J. Candy, B. N. Breizman, J. W. Van Dam, and T. Ozeki, "Multiplicity of low-shear toroidal Alfvén eigenmodes," *Phys. Lett. A*, vol. 215, pp. 299 – 304, 1996, doi:10.1016/0375-9601(96)00197-1.

[19] T. Hellsten and L. Villard, "Power deposition for ion cyclotron heating in large tokamaks," *Nucl. Fusion*, vol. 28, no. 2, pp. 285 – 295, 1988, doi:10.1088/0029-5515/28/2/009.

[20] T. O'Neil, "Collisionless damping of nonlinear plasma oscillations," *Phys. Fluids*, vol. 8, no. 12, pp. 2255 – 2262, 1965, doi:10.1063/1.1761193.

[21] M. B. Levin, M. G. Lyubarskiĭ, I. N. Onishchenko, V. D. Shapiro, and V. I. Shevchenko, "Contribution to the nonlinear theory of kinetic instability of an electron beam in plasma," *J. Exp. Theor. Phys.*, vol. 35, no. 5, pp. 898 – 901, 1972.

[22] H. L. Berk, B. N. Breizman, and M. S. Pekker, "Simulation of Alfvén-wave-resonant-particle interaction," *Nucl. Fusion*, vol. 35, no. 12, pp. 1713 – 1720, 1995, doi:10.1088/0029-5515/35/12/I36.

[23] H. L. Berk, B. N. Breizman, and M. Pekker, "Numerical simulation of bump-on-tail instability with source and sink," *Phys. Plasmas*, vol. 2, no. 8, pp. 3007 – 3016, 1995, doi:10.1063/1.871198.

[24] E. Tholerus, T. Hellsten, and T. Johnson, "The effects of phase decorrelation on the dynamics of the bump-on-tail instability," *Phys. Plasmas*, vol. 22, no. 8, p. 082106, 2015, doi:10.1063/1.4928094.